JACS
JOURNAL OF THE AMERICAN CHEMICAL SOCIETY

Communication

pubs.acs.org/JACS

A ^{18}F-Labeled Saxitoxin Derivative for *in Vivo* PET-MR Imaging of Voltage-Gated Sodium Channel Expression Following Nerve Injury

Aileen Hoehne,[∥,†] Deepak Behera,[∥,†] William H. Parsons,[∥,‡] Michelle L. James,[†] Bin Shen,[†] Preeti Borgohain,[†] Deepika Bodapati,[†] Archana Prabhakar,[†] Sanjiv S. Gambhir,[†] David C. Yeomans,[§] Sandip Biswal,*[,†] Frederick T. Chin,*[,†] and J. Du Bois*[,‡]

[†]Department of Radiology, [‡]Department of Chemistry, and [§]Department of Anesthesia, Stanford University, Stanford, California 94305, United States

Supporting Information

ABSTRACT: Both chronic and neuropathic pain conditions are associated with increased expression of certain voltage-gated sodium ion channel (Na_V) isoforms in peripheral sensory neurons. A method for noninvasive imaging of these channels could represent a powerful tool for investigating aberrant expression of Na_V and its role in pain pathogenesis. Herein, we describe the synthesis and evaluation of a positron emission tomography (PET) radiotracer targeting Na_Vs, the design of which is based on the potent, Na_V-selective inhibitor saxitoxin. Both autoradiography analysis of sciatic nerves excised from injured rats as well as whole animal PET-MR imaging demonstrate that a systemically administered [^{18}F]-labeled saxitoxin derivative concentrates at the site of nerve injury, consistent with upregulated sodium channel expression following axotomy. This type of PET agent has potential use for serial monitoring of channel expression levels at injured nerves throughout wound healing and/or following drug treatment. Such information may be correlated with pain behavioral analyses to help shed light on the complex molecular processes that underlie pain sensation.

Current clinical approaches for the diagnosis of chronic pain rely on subjective methods of analysis, which include patient self-reporting and physical exams.[1] Various imaging modalities such as X-ray, computed tomography (CT), and conventional magnetic resonance imaging (MRI) have limited utility for objectively identifying hypersensitive 'pain-generating' neural structures and accurately assessing pain syndromes.[2−5] Accordingly, *in vivo* methods to pinpoint discrete molecular and cellular changes associated with certain pain pathologies could greatly enhance our understanding of the molecular etiology of nociception and potentially offer impartial data to better inform patient care.

Voltage-gated sodium channels (Na_Vs), which play a fundamental role in the formation and conduction of action potentials in excitable tissue,[6] are of particular interest as molecular markers of pain. Certain Na_V isoforms are known to be upregulated in peripheral sensory neurons and dorsal root ganglia following neuronal or soft tissue injury, and have been causally linked to enhanced nociceptive activity.[7] Dysregulation of sodium channels can result in ectopic neuronal firing and neuronal hyperexcitability associated with neuropathic pain.[8] A method for noninvasive detection of Na_Vs could enable imaging experiments in living subjects that correlate changes in protein expression with sensitization to pain stimuli. Herein, we describe

Scheme 1. De Novo Synthesis of ^{19}F- and ^{18}F-Labeled Saxitoxins

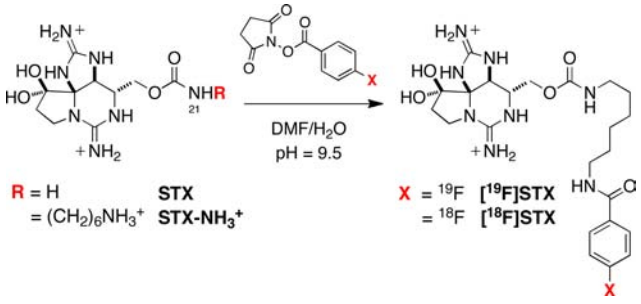

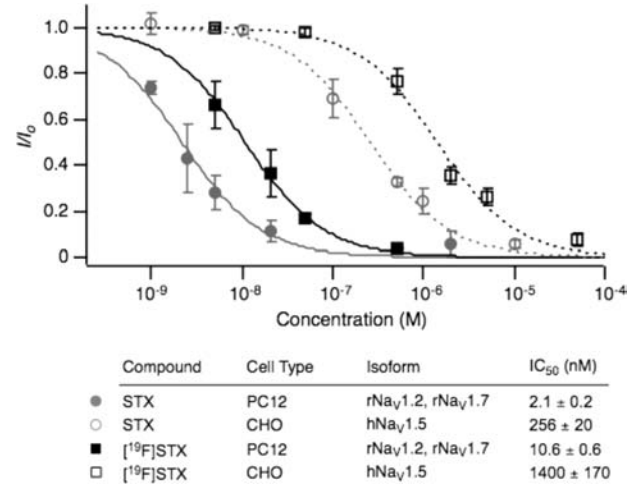

Figure 1. Concentration−response curves and IC_{50} values for STX (circles) and [^{19}F]STX (squares) tested against differentiated PC12 cells endogenously expressing TTX-sensitive $Na_V1.2$ and $Na_V1.7$ (filled), and CHO cells transiently expressing TTX-insensitive $Na_V1.5$ (hollow) [$n \geq 3$, error bars represent standard deviations; I/I_0 = remaining current/initial current]. Current versus time plots are shown in Figure S2 in the Supporting Information.

Received: August 10, 2013
Published: November 21, 2013

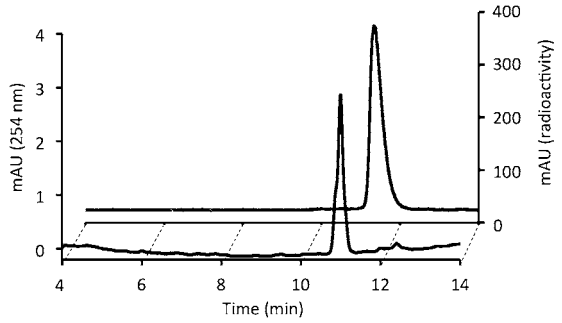

Figure 2. Analytical HPLC chromatogram of formulated [^{18}F]**STX** coinjected with [^{19}F]**STX**.

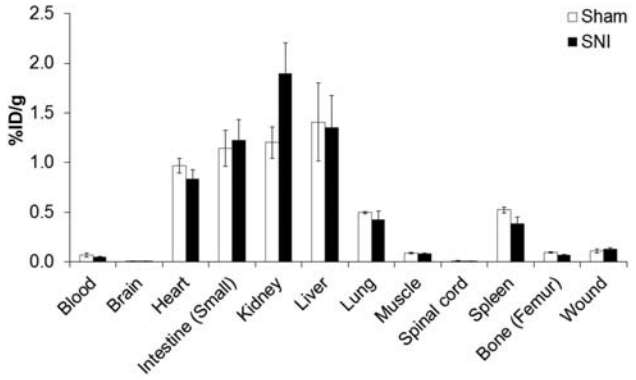

Figure 3. Biodistribution of [^{18}F]**STX** in sham-operated versus SNI rats. Tissues were collected at 60 min postinjection (p.i.), and associated radioactivity was measured with a gamma-counter (n = 3, error bars represent standard errors). Wound is defined as surgical damage to non-neural structures, including muscle and skin. Differences in uptake in nontarget tissues were not statistically significant.

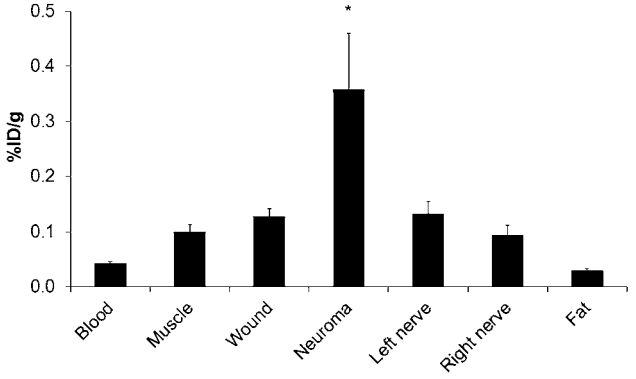

Figure 4. Uptake of [^{18}F]**STX** in the neuroma of SNI rats compared to background signal in representative nontarget tissues (*p < 0.05). Data collected at 60 min p.i. (n = 3, error bars represent standard errors).

our initial efforts to develop a positron emission tomography (PET) radiotracer for imaging peripheral nerve injury in an animal model of neuropathic pain by targeting overexpression of Na_Vs.

A number of small molecule and peptide ligands are known to bind Na_Vs selectively and could potentially serve as PET probes. Among this collection, saxitoxin (STX), a unique bis-guanidinium natural product, offers two salient features. First, STX binds reversibly and with low nanomolar affinity to the extracellular pore of tetrodotoxin (TTX)-sensitive Na_V isoforms[9] and, thus, has the advantage of a readily accessible target on the

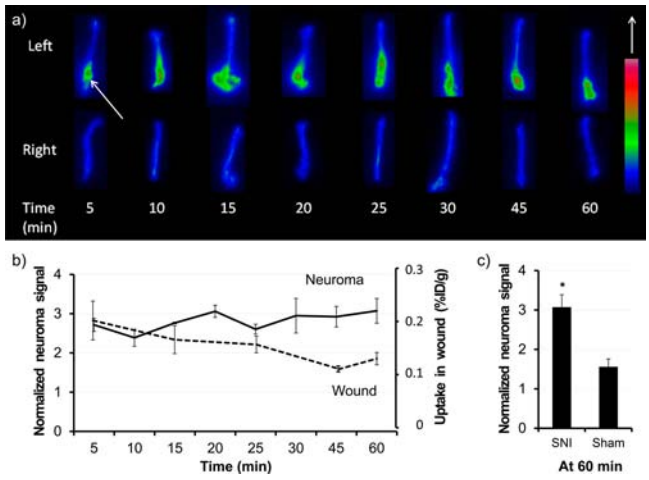

Figure 5. (a) Autoradiography of injured left sciatic and uninjured right sciatic nerves of SNI animals harvested at different time points postinjection. (b) Time plot of normalized signal in the neuroma over 60 min, determined by autoradiography, and coplotted with uptake in the surgical wound as determined in biodistribution studies. (c) Autoradiography signal in sciatic nerves of SNI and sham-operated animals at 60 min (n = 3; error bars represent standard errors; *p < 0.05). Normalized to control areas in the same nerve.

cell surface.[10] Second, prior studies have demonstrated that functional group substitutions at N21 in STX can be accommodated with minimal perturbation of the ligand–receptor binding interaction.[11] In particular, *N*-(aminohexyl)-STX (**STX-NH$_3^+$**), a compound prepared previously by our lab, can be conjugated to a variety of groups through selective amide bond formation.[12] Such a method enables final-step introduction of an appropriate radiolabel for PET imaging. Our radiolabel of choice, fluorine-18, offers both a half-life (109.8 min) compatible with the anticipated distribution kinetics of an STX-based radiotracer and a low positron energy, which affords optimal imaging resolution.[13]

Coupling of **STX-NH$_3^+$** with the *N*-hydroxysuccinimide ester of 4-fluorobenzoic acid ([^{19}F]**SFB**) furnished the corresponding benzamide ([^{19}F]**STX**) in 87% yield when 3.0 equiv of the ester were employed (Scheme 1). To optimize this coupling protocol for radiosynthesis by minimizing the amount of ester, this reaction was also examined using a 4-fold excess of **STX-NH$_3^+$** relative to [^{19}F]**SFB**. Under these conditions, [^{19}F]**STX** was obtained in 1 h in 88% yield; the uncoupled **STX-NH$_3^+$** was easily separated from the desired product by reversed-phase HPLC.

The affinity of [^{19}F]**STX** for Na_V was determined by measuring block of peak Na^+ current in whole-cell voltage-clamp experiments (Figure 1, Figure S2). Against nerve growth factor (NGF)-differentiated PC12 cells, which endogenously express two TTX-sensitive isoforms (rNa_V1.2 and rNa_V1.7),[14] the measured potency of the benzamide-modified toxin was only 5-fold less than that of the natural product (IC_{50} = 10.6 ± 0.6 nM for [^{19}F]**STX** and 2.1 ± 0.2 nM for native STX). Importantly, both STX and [^{19}F]**STX** were substantially less potent inhibitors of recombinant Na_V1.5 (CHO cells), a TTX-insensitive isoform expressed principally in heart tissue (IC_{50} = 256 ± 20 nM and 1.40 ± 0.17 μM, respectively). These results indicate that [^{19}F]**STX** binds to TTX-sensitive Na_Vs with high affinity and with a channel subtype selectivity profile similar to the parent molecule.[15]

Radiolabeled STX was prepared from [^{18}F]**SFB**, a reagent commonly used for generating ^{18}F PET probes (Scheme 1). A

dx.doi.org/10.1021/ja408300e | J. Am. Chem. Soc. 2013, 135, 18012–18015

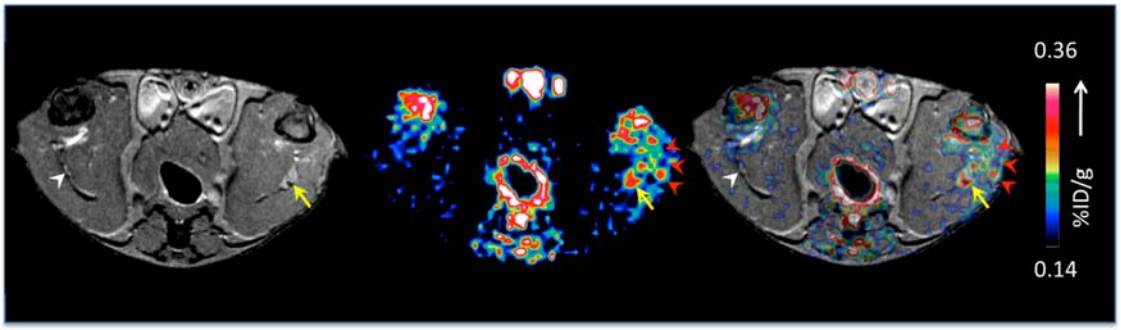

Figure 6. Representative cross-sectional MR, PET, and fused PET-MR (left to right) image of the thighs showing the transverse plane through the neuroma of a spared nerve injury (SNI) rat comparing [^{18}F]**STX** uptake in the injured left sciatic nerve (yellow arrow) versus the uninjured right nerve (white arrowhead). Red arrowheads: uptake in the wound. PET signal (normalized to signal from adjacent muscle) in the left nerve was 1.56 ± 0.29, n = 5, and 1.11 ± 0.14 on the control side; $p < 0.05$. As expected, increased PET signal is also observed in the urinary and excretory systems as well as the knee joints.

semiautomated procedure for this synthesis was developed from a conventional protocol[16,17] (Figure S3) and provided [^{18}F]**SFB** in 31.1 ± 12.4% radiochemical yield (n = 26), decay-corrected from end of bombardment. Following treatment of [^{18}F]**SFB** with **STX-NH$_3^+$** (Scheme 1), the product [^{18}F]**STX** was purified by semipreparative HPLC and formulated in PBS (Figure 2). When 200−250 μg of **STX-NH$_3^+$** were employed in the coupling step, the desired product was generated in radiochemical yields of 6.6 ± 3.7% (from [^{18}F]**SFB**, n = 8); however, when the amount of **STX-NH$_3^+$** was elevated to 500 μg, radiochemical yields of [^{18}F]**STX** increased to 16.4 ± 9.5% (from [^{18}F]**SFB**, n = 12). Using this latter procedure, the overall synthetic efficiency and the specific activity of the radiotracer (1.63 ± 1.14 Ci/μmol; 60.3 ± 42.2 GBq/μmol; n = 12) were improved. Ultimately, [^{18}F]**STX** was obtained after a total synthesis time of 3−3.5 h from end-of-bombardment with a radiochemical purity of ≥93%. The successful synthesis of [^{18}F]**STX** represents a rare example of a complex natural product derivative incorporating a fluorine-18 isotope.[18]

Evaluation of [^{18}F]**STX** for PET imaging of neuromas was performed with rats having undergone a spared-nerve injury (SNI) surgical procedure. SNI is a validated experimental model of neuropathic pain that involves transection of the tibial and common peroneal branches of the sciatic nerve, leaving the sural branch intact. This procedure introduces a neuroma at the site of nerve injury and produces chronic pain lasting several months.[19] In our studies, an allodynic response in the left hind paws (operated side) of SNI animals was confirmed four weeks postsurgery using von-Frey filaments (Figure S5). Immunohistopathology data of the surgically injured nerve of SNI animals show elevated levels of protein expression of $Na_V1.3$ and $Na_V1.7$ as compared to the control.[20,21]

The metabolic stability of our STX tracer was confirmed through HPLC analysis of urine samples taken from SNI animals 60 min postinjection (p.i.) of [^{18}F]**STX**. In this experiment, 968 μCi [^{18}F]**STX** with a specific activity of 1.1 Ci/μmol (40.4 GBq/μmol) at the time of injection was administered to the rat (300 g). As expected given the small amount of tracer injected [0.47 μg (0.90 nmol)] and the reduced potency of [^{19}F]**STX** compared to native STX (LD50 7 μg/kg, 23 nmol/kg),[22] no signs of toxicity were observed in either this experiment or subsequent studies using lower mass doses. Analysis of the rat urine showed that 97% of the radioactive material had a retention time identical to that of [^{18}F]**STX** (Figure S6), indicating that the radiotracer suffers little if any degradation systemically or in the renal system.[23]

In order to gain an understanding of the distribution kinetics of [^{18}F]**STX**, tissue-associated radioactivity levels were determined at serial time points following intravenous injection of the radiotracer (Table S1). Animals were euthanized at 5, 10, 15, 30, 45, and 60 min postinjection of [^{18}F]**STX**, and tissues were collected, weighed, and analyzed for radioactivity with a gamma-counter. Organs with higher levels of absolute uptake (above 1% ID/g) included heart, small intestine, kidney, and liver. Low tracer uptake in muscle (0.07−0.10%ID/g) and rapid blood clearance (0.19%ID/g at 5 min p.i. to 0.05%ID/g at 60 min p.i.) were noted, both of which favor minimal background signal in PET imaging. The uptake in brain was quite low (~0.1%ID/g) and consistent with our expectation that the dicationic [^{18}F]**STX** should not cross the blood−brain barrier. Radioactivity levels in bone were also ~0.1%ID/g and constant over 60 min, indicating negligible defluorination of the benzamide moiety. Comparison of the results from both SNI and sham-operated animals at 60 min p.i. confirmed that nerve injury does not alter radiotracer distribution in nontarget tissues (Figure 3).

Consistent with our expectation, increased uptake of [^{18}F]**STX** was observed in the neuroma (0.36 ± 0.18%ID/g at 60 min postinjection). Adjacent wound tissue, on the other hand, retained only 0.13 ± 0.02%ID/g (Figure 4). Further, tracer levels in the neuroma were 3.8-fold higher than in the normal (or uninjured) right sciatic nerve (0.09 ± 0.03%ID/g). Radiotracer retention in the neuroma was confirmed by *ex vivo* autoradiography of the injured and uninjured sciatic nerve segments excised at multiple time points over a 1 h period. At 60 min following injection, the normalized tracer uptake (determined from autoradiography images) in the neuroma of SNI animals was higher than that in sham-operated animals (3.07 ± 0.54 vs 1.56 ± 0.28; $F(2,6) = 13.6$; $p < 0.01$, Figure 5c). In addition, [^{18}F]**STX** retention in the neuroma remained constant over time ($p > 0.05$, Figure 5a). Collectively, these data provide support for specific [^{18}F]**STX** uptake in the neuroma compared to the surrounding tissue (Figure 5b).[24]

Encouraged by the results of our *ex vivo* experiments, we performed preliminary PET scans of SNI rats with [^{18}F]**STX** using MRI for anatomic correlation. Since current small-animal PET scanners are limited by their relatively poor spatial resolution,[25] it is difficult to identify peripheral nerves using only PET. MRI offers greater spatial resolution and has been used in conjunction with PET for anatomic localization. By coregistering images from both modalities, the excellent spatial and soft-tissue contrast resolution of MRI can be leveraged with

the high sensitivity of PET to locate radiotracer signal in the sciatic nerve.

Results from the PET-MRI studies revealed increased [^{18}F]**STX** uptake in the left injured nerve of SNI animals (Figure 6, PET signal (normalized to signal from adjacent muscle) 1.56 ± 0.29, n = 5). By contrast, the uninjured sciatic nerve showed reduced signal (normalized PET signal 1.11 ± 0.14 on the control side; $p < 0.05$). These initial data demonstrate the feasibility of using [^{18}F]**STX** PET to investigate sodium channel levels and distribution in disease states.

We have successfully prepared a radiolabeled form of a potent sodium channel antagonist to generate a novel PET tracer, [^{18}F]**STX**. Elevated concentrations of [^{18}F]**STX** are detected at the location of nerve injury in an animal model of neuropathic pain. Our work represents one of the first attempts to mark Na_Vs in an intact, living animal model.[26] We envision using this type of PET agent for serial monitoring of changes in channel expression levels that occur at injured nerves as a function of wound healing and/or drug treatment. Such information may be correlated with pain behavioral analyses to help shed light on the complex molecular processes that underlie pain sensation.

■ ASSOCIATED CONTENT

Supporting Information

Experimental details, supplementary figures and table. This material is available free of charge via the Internet at http://pubs.acs.org.

■ AUTHOR INFORMATION

Corresponding Authors

biswals@stanford.edu
chinf@stanford.edu
jdubois@stanford.edu

Author Contributions

‖A.H., D.B., and W.P. contributed equally.

Notes

The authors declare the following competing financial interest(s): Three of the authors, Yeomans, Biswal, and Du Bois, are cofounders and hold equity shares in SiteOne Therapeutics, Inc., a start-up interested in developing diagnostic probes for pain and novel medicines for pain treatment.

■ ACKNOWLEDGMENTS

The authors would like to thank Dr. John Mulcahy and Dr. Stephanie Torreilles for their assistance with the animal studies as well as the Stanford Small Animal Imaging Facility. This project was supported in part by a Stanford University Bio-X Grant (S.B., J.D.B.) and NIH R01 NS045684 (J.D.B.), and by the NCI ICMIC P50 Grant CA114747 (S.S.G.). W.H.P. was supported as a Stanford Interdisciplinary Graduate Fellow (SIGF).

■ REFERENCES

(1) Institute of America (U.S.) Committee on Advancing Pain Research Care and Education, in *Relieving Pain in America: A Blueprint for Transforming Prevention, Care, Education and Research*, Washington D.C., 2011.

(2) Englund, M.; Guermazi, A.; Gale, D.; Hunter, D. J.; Aliabadi, P.; Clancy, M.; Felson, D. T. *N. Engl. J. Med.* **2008**, *359*, 1108−1115.

(3) Elfering, A.; Semmer, N.; Birkhofer, D.; Zanetti, M.; Hodler, J.; Boos, N. *Spine* **2002**, *27*, 125−134.

(4) Vetti, N.; Krakenes, J.; Ask, T.; Erdal, K. A.; Torkildsen, M. D. N.; Rorvik, J.; Gilhus, N. E.; Espeland, A. *Am. J. Neuroradiol.* **2011**, *32*, 1836−1841.

(5) Srinivas, S. V.; Deyo, R. A.; Berger, Z. D. *Arch. Intern. Med.* **2012**, *172*, 1016−1020.

(6) Hille, B. *Ion Channels of Excitable Membranes*, 3rd ed.; Sinauer Associates: Sunderland, MA, 2001.

(7) Rogers, M.; Tang, L.; Madge, D. J.; Stevens, E. B. *Sem. Cell Devel. Biol.* **2006**, *17*, 571−581.

(8) Dib-Hajj, S. D.; Black, J. A.; Waxman, S. G. *Pain Med.* **2009**, *10*, 1260−1269.

(9) Fozzard, H. A.; Lipkind, G. M. *Mar. Drugs* **2010**, *8*, 219−234.

(10) Morse, D. L.; Gillies, R. J. *Biochem. Pharmacol.* **2010**, *80*, 731−738.

(11) Andresen, B. M.; Du Bois, J. *J. Am. Chem. Soc.* **2009**, *131*, 12524−12525.

(12) Ondrus, A. E.; Lee, H. D.; Iwanaga, S.; Parsons, W. H.; Andresen, B. M.; Moerner, W. E.; Du Bois, J. *Chem. Biol.* **2012**, *19*, 902−912.

(13) Lasne, M.-C.; Perrio, C.; Rouden, J.; Barré, L.; Roeda, D.; Dolle, F.; Crouzel, C. *Top. Curr. Chem.* **2002**, *222*, 201−258.

(14) D'Arcangelo, G.; Paradiso, K.; Shepherd, D.; Brehm, P.; Halegoua, S.; Mandel, G. *J. Cell Biol.* **1993**, *122*, 915−921.

(15) [^{19}F]**STX** also binds with nanomolar potency to Na_V1.4 (Figure S2). We anticipate that it should bind with nanomolar affinity to Na_V1.1, 1.3, and 1.6, which are TTX-sensitive.

(16) Tang, G.; Zeng, W.; Yu, M.; Kabalka, M. *J. Label. Compd. Radiopharm.* **2008**, *51*, 68−71.

(17) Tang, G.; Tang, X.; Wang, X. *J. Label. Compd. Radiopharm.* **2010**, *53*, 543−547.

(18) Recent examples of other ^{18}F-labeled natural products: (a) Kiesewetter, D. O.; Jagoda, E. M.; Kao, C.-H.; Ma, Y.; Ravasi, L.; Shimoji, K.; Szajek, L. P.; Eckelman, W. C. *Nucl. Med. Biol.* **2003**, *30*, 11−24. (b) Lee, E.; Kamlet, A. S.; Powers, D. C.; Neumann, C. N.; Boursalian, G. B.; Furuya, T.; Choi, D. C.; Hooker, J. M.; Ritter, T. *Science* **2011**, *334*, 639−642. (c) Lee, J. H.; Peters, O.; Lehmann, L.; Dence, C. S.; Sharp, T. L.; Carlson, K. E.; Zhou, D.; Jeyakumar, M.; Welch, M. J.; Katzenellenbogen, J. A. *Nucl. Med. Biol.* **2012**, *39*, 1105−1116.

(19) Decosterd, I.; Woolf, C. J. *Pain* **2000**, *87*, 149−158.

(20) Black, J. A.; Cummins, T. R.; Plumpton, C.; Chen, Y. H.; Hormuzdiar, W.; Clare, J. J.; Waxman, S. G. *J. Neurophysiol.* **1999**, *82*, 2776−2785.

(21) Persson, A.-K.; Gasser, A.; Black, J. A.; Waxman, S. G. *Exp. Neurol.* **2011**, *230*, 273−279.

(22) Kohane, D.; Lu, N. T.; Gögköl-Kline, A. C.; Shubina, M.; Kuang, Y.; Hall, S.; Strichartz, G.; Berde, C. B. *Reg. Anesth. Pain Med* **2000**, *25*, 52−59.

(23) Hagenbuch, B. *Clin. Pharmacol. Ther.* **2010**, *87*, 39−47.

(24) In order to demonstrate the specificity of the observed uptake further, we attempted to block radiotracer binding by coinjection with an excess of [^{19}F]**STX**. For details about this experiment refer to Figure S8 and the supplementary discussion in the Supporting Information.

(25) Weber, S.; Bauer, A. *Eur. J. Nucl. Med. Mol. Imaging* **2004**, *31*, 1545−1555.

(26) Pérez-Medina, C.; Patel, N.; Robson, M.; Lythgoe, M. F.; Årstad, E. *Bioorg. Med. Chem. Lett.* **2013**, *23*, 5170−5173.